

NUMERICAL AND EXPERIMENTAL STUDY OF WIND LOAD AROUND BUILDINGS OF DIFFERENT HEIGHTS

N.M. Guirguis¹ M.M. Nassief²

ABSTRACT

A three-dimensional study is performed experimentally and numerically to investigate the effect of wind pressure on different surfaces of buildings.

A simple test model was designed and constructed using Perspex material. The model was tested through a wind and a smoke tunnel in the Housing and Building Research Center (HBRC), Cairo – Egypt . The test model has a facility to change its direction with the airflow ($\alpha=0^\circ, 30^\circ, 60^\circ, 90^\circ, 120^\circ, 150^\circ, 180^\circ$). The used program is a computer software package, namely (ANSYS CFD FLOTRAN) was acquired and used in the present work. This program solves the flow fields in any given domain using the finite element method. A model was created in three-dimensional with maximum number of nodal points of 50000, with tetrahedral elements. The results were presented as velocity and pressure contours. Also the effect of building height, wind speed and wind angle on pressure distribution was predicted. A good agreement between the experimental and theoretical results is obtained.

KEYWORDS Wind Tunnel – Smoke Tunnel- Wind Load- Pressure Coefficient - ANSYS CFD Flotran

NOMENCLATURE

C_p : Pressure coefficient.
 P : Surface pressure, Pa.
 P_d : Dynamic pressure ($= \rho v^2/2$), Pa.
 P_s : Static pressure at the tunnel surface beside the test model, Pa.
 x_i, x_j : The coordinates, m.
 u_i : Velocity component u, v, w ($i=1,2,3$), m/s.
 u_j : Velocity component u, v, w ($j=1,2,3$), m/s.
 u, v, w : Components of the velocity-vector in x,y,z directions, respectively.
Y/H : Dimensionless pressure tap location at the model center line

ρ : Fluid density (constant) , kg/m³.
 μ : Dynamic viscosity, Pa.s.
 μ_t : Turbulence or eddy viscosity, Pa.s.
 \mathcal{K} : Kinetic energy, J.
 δ_{ij} : Constant =1 for $i=j$ and =zero for $i \neq j$

INTRODUCTION

Wind loads have to be taken into account when designing engineering structures. The wind load on structures can be systematized by means of the wind load chain: wind climate (global wind), terrain (wind at low height), aerodynamic response (wind flow to pressure), mechanical response (wind pressure to structural response) and design criteria. The dynamic wind load covers vibrations induced by wind turbulence, vortex shedding, and flutter and galloping. Buildings having even moderately complex shapes, such as L-or U- shaped structures formed by two or three rectangular blocks, can generate flow patterns too complex to generalize for design. To determine flow conditions influenced by surrounding buildings or topography, wind tunnel or water channel tests of existing building are required. A stagnation zone exists on the upwind wall. The flow separates at the sharp edges to generate a recirculation flow zones that cover the downwind surface of the building (roof, sides, and leeward walls) and extend for some distance into the wake as shown in Fig. (1). If the building has sufficient length L in the windward direction, the flow will reattach to the building and may generate two distinct regions of separated recirculation flow on the building and in its wake. Surface flow pattern on the upwind wall are largely influenced by approach higher wind speed at roof level causes a larger stagnation pressure on the upper part of the wall than near the ground, which leads to down wash on the one-half to two-thirds of the building. This ground level upwind vortex is carried around the sides of the building in a U shape and is responsible for the suspension of dust and debris that can contaminate air intakes close to ground level. Streamline patterns are independent on wind

speed and depend mainly on building shape and upwind condition, ASHRAE [2].

Shaanan, et al [6] gave wind tunnel results of testing a series of rectangular cross section obstacles placed on tunnel floor and immersed in an air stream using turbulence and velocity grids to simulate atmospheric surface layer. Single and series-arranged obstacles were tested, also side by side obstacles and series arranged rows of these obstacles were examined. Velocity profile, turbulence profile, and pressure distribution on tunnel floor (representing ground in nature) were measured under various wind conditions when blowing at right angles to the obstacle face. The work was carried out principally to investigate fencing characteristics for sand dune control. The models tested may still be considered to correspond to single buildings and building groupings (mainly the two dimensional case) and the data obtained could be useful and applicable to building studies.

Cermak [3] described tests carried out on building models in a long test section in closed and open circuit wind tunnel. Four common types of small scale models were used for tests to yield data for design and analysis. Data from these tests were recommended by the author to be used with wind data obtained from a meteorological station near the construction site.

Daryl, et al [4] identifies some common sources of torsional loading in terms of building shape, interfering effect of nearby buildings and dynamic characteristics of the structure frame. All models were tested in a wind tunnel. It is shown that the torsional loading is routinely larger than that provided for in most standards.

Stathopoulos, et al [7] studied wind pressure on buildings with stepped roofs. In their paper, they described an experimental study for the evaluation of wind pressure on buildings with roofs of two different heights, such as one building with roofs at two levels or, more commonly, two flat roofed buildings in a row. Extensive series of tests were carried out in a boundary layer wind tunnel simulating the flow over an open country terrain exposure. The maximum height of the model was variable and could represent a building up to 60 m high. The results of the study for buildings with a two level flat roof were discussed. Data were presented as pressure coefficients. The results of the study were compared with the flat roof specifications described in the American National Standard Institute Wind Standards and the National building code of Canada, showing that some modifications of these standards were required to accommodate the wind loading of this building configurations. In particular, positive pressure coefficients must, according to the authors, be considered for stepped roofs.

Hassan, [5] in cooperation with the first author has studied a building model in a wind tunnel. This model was subjected to a series of tests including measurements of pressure distributions on its different exposed surfaces (front, rear side, and roof) for different wind speeds ranging from 3.8 m/s to 14.3 m/s and wind directions ranging from 0 to 180. He concluded that the velocity and turbulent grids mounted at tunnel entrance gave a good logarithmic velocity profile as in nature wind. He also concluded that wind conditions (mean speed, direction, turbulence, and velocity profile) appear to have significant influences on the flow

characteristics around the exterior surfaces of a typical building.

In this paper, the main interest is to predict the wind loads on different side walls of different model's height. The study doesn't include the pressure on the roof since the effect of wind pressure and direction on the roof have no significant effect since the wind direction is parallel to the roof.

Karakatsanis, et al [8] gave wind pressure coefficients at various openings of a wind tower determined by testing a scale model of the building in a boundary layer wind tunnel. (Wind towers are structures employed in Iran and neighboring countries for natural ventilation and passive cooling). Tests were conducted on an isolated tower, then on tower and an adjoining house, then on tower and house surrounded by a courtyard. The wind pressure coefficients at the tower and house openings were determined at various wind angles for two types of terrain: suburban and open country. The airflow rates were then estimated from knowledge of wind pressure coefficients at the building aperture. It was concluded that the presence of a courtyard around the structure and the angle of incidence of the wind both influence the rate and direction of air flowing from the tower into the house. If leeward openings of the tower could be closed (for example, by automatic dampers) restricting the air leaving these apertures, the airflow rate from the tower to the house could be greatly increased. The results of this investigation were believed to provide assistance to architects and engineers in the design of wind towers for the desired ventilation rates in buildings.

Baskaran [9] developed a computational fluid dynamics CFD program to predict the wind environmental conditions around buildings. This CFD program have been applied in predicting wind flow conditions: around a single building, between two parallel buildings and around a multiple building configuration. Also presented is a limited model validation for those simulated configurations. Also he presented the application of CFD program for a case study in simulating an existing site together with proposed buildings and the local landscape.

Delaunay, et al [10] investigated the gas dispersion around a rectangular building placed in a simulated atmospheric boundary layer. Numerical simulations of these experiments have been performed by solving the Reynolds-averaged Navier-Stokes equations, combined with a Reynolds-stress turbulence model. The calculated values of gas concentrations on the building model faces agree generally well with measurements.

Yaghoubi, [11] used a computer simulation to obtain the flow patterns around and through simple rectangular buildings, with and without apertures, singly or in series, with varying aspect ratio and spacing. Flow parameters, including velocity vectors, streamlines, pressure contours and locations of separation and reattachment are developed for different Re. The ventilation rates are affected by the flow interaction between buildings.

In the **Egyptian code, [12]** the total wind force on the building as a whole is calculated on the whole building instead of calculating it on a unit area of the building especially the building in which its height ratio to its other dimensions is very large.

From the site ref. [13], the normal force network is used to calculate the design wind pressure for different surfaces of a building which depends on combined height, exposure factor coefficient, wind stagnation pressure, importance factor and pressure coefficient.

The site ref. [14], shows that the wind pressure has its value due to its velocity. As the air passes over and round thr building, the pressure are positive on the windward side and negative on the lee or sheltered side. It is often the negative pressures that suck roofs off buildings and windows of walls. When wind is stopped, its velocity pressure is converted into static pressure.

EXPERIMENTAL WORK

In order to study the wind pressure around buildings, different test models with different heights were fabricated and tested in a wind tunnel. Figures (2,a-b) show a layout of the wind tunnel (designed and built at the Housing & Building Research Center, HBRC). Also a scale models were tested inside a smoke tunnel to observe and photograph the airflow configuration around these models. The smoke tunnel provides a simple picture of turbulence, stagnation and reattachment zones around building models. A Photograph and a schematic diagram of the smoke tunnel is shown in Fig.(3). Figure (4) shows a schematic of the test model, and table (1) shows the dimension of the test models. The test model, was made from plastic sheet (Plexiglas 0.003 m thick) of dimension: 0.01 m x 0.01 m base x (variable highs: 0.05, 0.10, 0.15, 0.20 and 0.25 m). These test models were provided with pressure taps on its wall surfaces. The pressure distribution around building model was measured inside the wind tunnel by using a data acquisition system outside the wind tunnel.

THEORETICAL WORK

Three general assumptions are assumed, these are the fluid is Newtonian, the flow is a single-phase one, the solution domain is of constant geometry, in addition, the flow is steady incompressible and the body forces are neglected. The continuity equation is the mathematical statement of the principle of conservation of mass, and can be expressed for steady incompressible-fluid flow as follow :

$$\frac{\partial u}{\partial x} + \frac{\partial v}{\partial y} + \frac{\partial w}{\partial z} = 0 \quad (1)$$

The momentum equation of motion in tensor form for 3-D turbulent flow is given by:

$$\frac{\partial}{\partial x_i}(u_i u_j) = -\frac{1}{\rho} \frac{\partial P}{\partial x_j} + \frac{1}{\rho} \frac{\partial}{\partial x_i} \{ (\mu + \mu_t) \left(\frac{\partial u_i}{\partial x_j} + \frac{\partial u_j}{\partial x_i} \right) - \frac{2}{3} \delta_{ij} \kappa \} \quad (2)$$

To obtain a solution of the above governing equations, boundary conditions related to the physical model under consideration must be specified as no slip condition is assumed to occur at all solid boundaries (building surfaces & ground). Thus the flow velocity is set to zero at these boundaries and the velocity profile of the undisturbed flow (upstream of the building model) is prescribed uniform.

Details of the solution of the above governing equations, based on introduction of the K- ϵ turbulence modeling and eddy viscosity approach are given in ANSYS (1). Figure (5) shows the applied boundary conditions.

RESULTS AND CONCLUSIONS

Theoretical Results :

In this analysis the code "ANSYS " is used to predict the flow characteristics around the building .

Figure (6) describes the velocity and pressure contours for various models of different heights (from H=0.05 m to H=0.25 m). For the velocity contours it is clear that as the building height increases the areas of the smaller velocities increase especially behind the building due to the formation of wakes. So as the height of the building increase the zone of wakes increases. For the pressure contours, the areas of larger pressure increase as the height of the building increases especially at the front of the building (stagnation zone) and vice versa for the back of building. Also, it is noticed that the two side walls and roof have a smaller values of pressure than the building's front, since the flow being parallel to these surfaces.

Figures (7) to (11) describe the effect of direction of flow with the height of building on both velocity and pressure contours. At angle 0° the windward wall lies in the stagnation zone (high pressure and low air velocity). Also as the air flow direction increases from 0° to 90°, the pressure coefficient decreases to reach its minimum value at angle 90° since the air flow is parallel to the wall, then the pressure is slightly increases till angle 180° due to the formation of eddies and recirculation flow .

Experimental Results :

The following results give relation between surface pressure coefficients and building height, wind speed and direction, where the surface pressure coefficient C_p can be calculated from the relation defined as:

$$C_p = (P - P_s) / P_d \quad (3)$$

Figure (12-a,b and c) shows the Visualization of flow around building models , with different angles (0, 30 , 60 deg.) for height H=0.10 m. From the figure it is noticed that the stagnation region (zero velocity and max. pressure) lies from the model base to about 2/3rd of the model height ,also the figure shows the recirculation regions (at the front and behind the model), it is obvious that the area of recirculation region behind the model is bigger than the corresponding on the front of the model.

Figure (13 - a, b, c, d and e) show flow visualization for building models of different heights (0.05, 0.10, 0.15, 0.20 and 0.25 m) and illustrates that as the height of the model increases the stagnation region position increases in height.

Figure (14) shows the centerline pressure coefficient for different wind angle (0°,30°,60°,90°,120°,150° and 180°) and different building height (0.05, 0.10, 0.15, 0.20 and 0.25 m). It is illustrated that the lowest pressure is at H = 0.05 m and as height increases the pressure increases till H = 0.15 m, then the model height has no effect on pressure. Also all the models at air flow angle 60° have an average pressure value lying between values at angles 30° and 90°, the angle

changing from 90° to 180° did not affect the pressure. Also it is clear that the maximum pressure for all models occurs at air flow angle 0°.

Figure (15) shows the average pressure variation with air flow angle for different building height. It is obvious that as the height of building increases the pressure increases and the angle 90° leads to the lowest pressure distribution for all models since the wind is perpendicular to that surface.

Figure (16) shows the effect of wind velocity on pressure variation with air flow angle for H = 0.25 m. It is clear that as the velocity increases the pressure decreases till angle 90° (the lowest value) then it increases till angle of 180°. Also for angle larger than 90° the pressure is almost constant for the higher velocities. It is noticed that whatever the value of the velocity of the wind is, the pressure is almost the same at angle 60°. Finally it is also noticed that as the air flow velocity increases, the difference between maximum and minimum values of Cp increases.

Figure (17) shows a comparison between theoretical and experimental results for pressure coefficient ($c_{p,av}$) for model height equal to 0.25 m and wind speed equal to 9 m/s. Fair agreement between them is clear with an average error of about ±20 %.

UNCERTAINTY ANALYSIS

A more precise method of estimating uncertainty in experimental results has been presented by Kline & McClintock, which is described in HOLMAN [15]. The relative error ($\partial u_{C_p} / \partial C_p$) for the pressure coefficient Cp can be expressed by the formula;

$$\frac{\partial U_{C_p}}{\partial C_p} = \left[\frac{\partial C_p}{\partial P} (U_P)^2 + \frac{\partial C_p}{\partial u} (U_u)^2 \right]^{1/2} \quad (4)$$

From the measurement data the relative error is equal to ±0.002

CONCLUSIONS

- 1) The pressure is higher in the front of the building model and decreases toward side walls and back wall.
- 2) The velocity approaches zero in the front of the model and has its higher value at the roof and side walls.
- 3) The stagnation region (zero velocity and max. pressure lies approximately at 2/3rd of the model height).
- 4) It is obvious that the recirculation region behind the model is larger than that at the front of the model.
- 5) As the air flow angle with the wall increases, the air velocity attached to the wall increases and the pressure decreases.
- 6) As the model height increases, the pressure increases and at flow angle 90° the pressure attains its lowest value for all models.
- 7) The effect of wind direction on the roof behavior is negligible, since it is always being parallel to the building roof.
- 8) There is a good agreement between the experimental and theoretical results.

REFERENCES

- 1- ANSYS, "FLOTRAN Analysis Guide", ANSYS, Inc. 1997.
- 2- ASHRAE, fundamental handbook, pp.14.1-14.18, 1989.
- 3- Cermak, J. E. " Wind tunnel modeling for structural design " , ACI structural journal , Vol. 86, No. 4 , pp. 592-600 , Sept. – Oct. , 1989.
- 4- Daryl, W. B., Noriaki, H. and Leighton, C. " Sources of torsional wind loading on tall buildings", Advanced technology of structure engineering (proceeding of the 2000 Structure Congress & Exposition, May, 2000, Philadelphia) ed. M. Elgaaly, SEI/ASCE, 2000.
- 5- Hassan, M. A., "Effect of wind speed and direction on the convective heat transfer coefficient on the external surfaces of building" M.Sc. Thesis, Cairo University, 1997.
- 6- Shaalan, M. R., shibl, A. M., and khoshaim, b. h. "An investigation of shelter characteristics of model fences", Journal of Engineering Science, King Saudi university, vol .9, pp.73-90, 1983.
- 7- Stathopoulos and Dumitrescu "Design recommendation for wind loading on building of intermediate highs" Canadian Journal , Dec., 1989.
- 8- Karakatsanic, C., Bahadori, M. N., and Viery, B. J., "Evaluation of Pressure Coefficient and Estimation of AirFlow Rates in Buildings Employing Wind Tower", Energy Vol. 37, No. 5, pp. 363-374, 1986.
- 9- Baskaran Appuollai and Kashef Ahmed, "Investigation of Air Flow Around Buildings Using Computational Fluid Dynamics Techniques", Engineering- Structures, Vol. 18, No. 11, pp. 861-875, Nov. 1996.
- 10- Delaunary, D., Lakehal, D., Barre, C., and Sacre, C., "Numerical and Wind Tunnel Simulation of Gas Dispersion around a Rectangular Building", Journal of Wind Engineering and Industrial Aerodynamics, Vol. 67-68, pp. 721-732, Apr.-Jun., 1997.
- 11- Yaghoubi, M., Zamanakhan, P., and Sabzevari, A., "Numerical Analysis of Two-Dimensional Wind Flow in and around Rectangular Buildings, Part II.
- 12- Egyptian Code for Calculating the Loads and Forces in Buildings Code No. 202, Jan. 2004, HBRC, EGYPT.
- 13- Wind Design Pressures for Your Building, http://WWW.timber.ce.wsu.edu/Supplements/WindDesign/wind_loads.html
- 14- Wind Pressure & Flow Around Buildings, Vent-Axia, WWW.vent-axia.com/sharing/windflow.asp
- 15- Holman, J. P. (1984), "Experimental Method for Engineers". 4th Edition McGraw hill Book Company, New York.

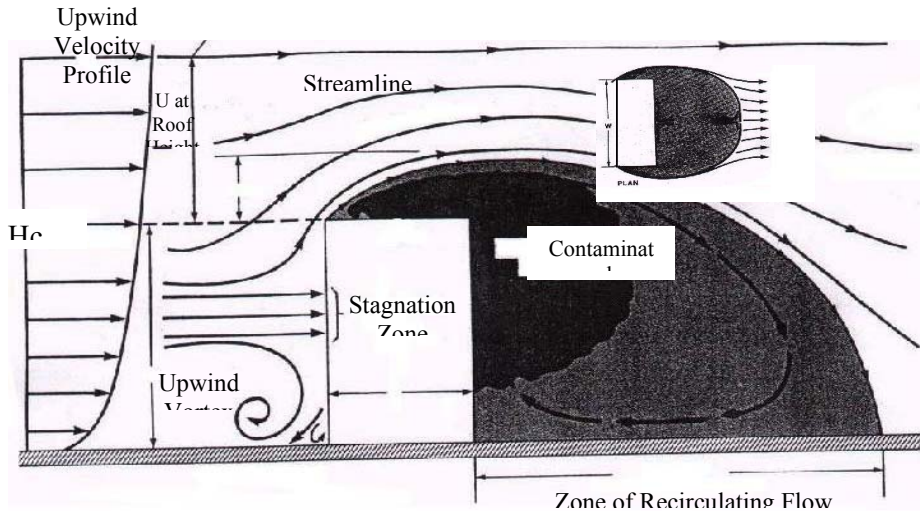
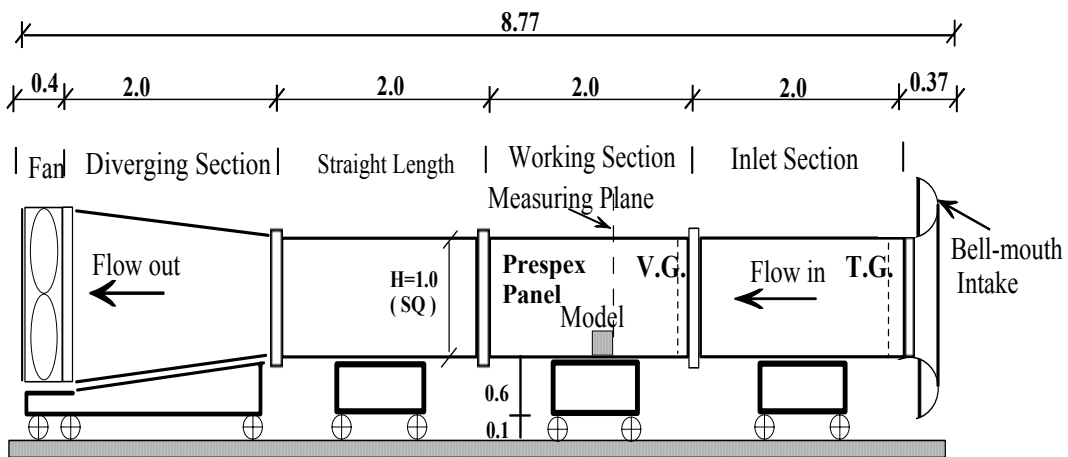


Fig. (1) : Building flow zones



Fig.(2-a) : A Photograph of the Wind Tunnel



**Fig. (2-b) : Wind tunnel layout showing location of turbulence and velocity grids relative to model
(Dim. in m).**

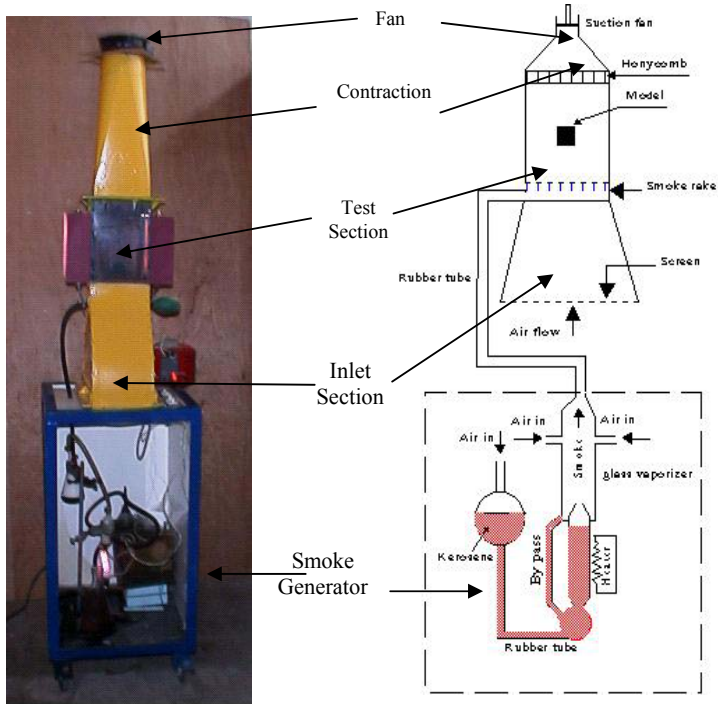


Fig. (3): Photo and schematic diagram Smoke tunnel details

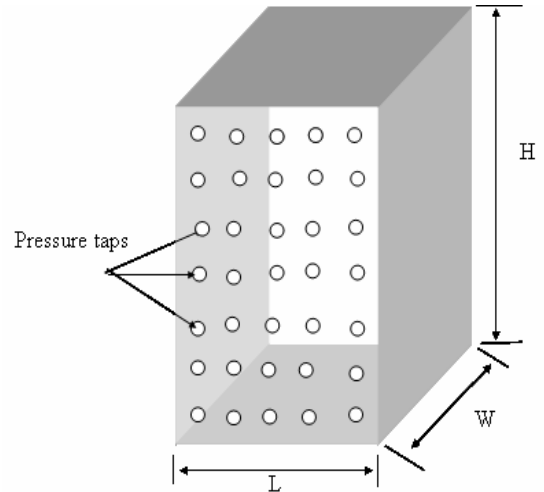


Fig. (4) : The test model.

Table (1): Dimension of the test models.

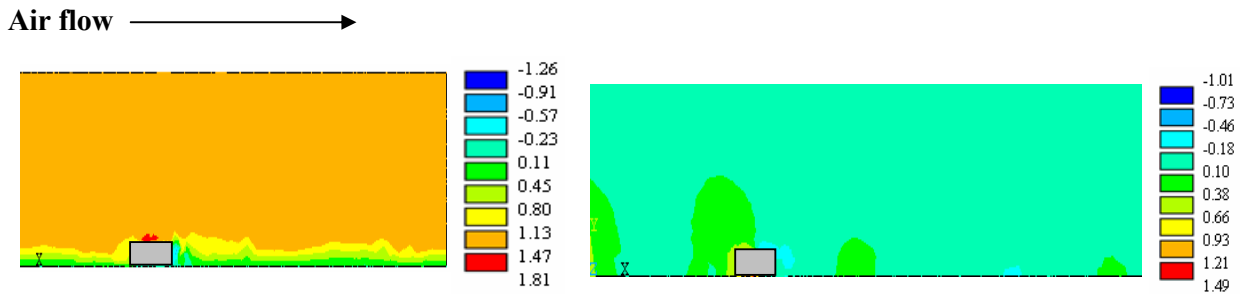
| Models | H (m) | L (m) | W (m) | Exp. | Theo. |
|--------|-------|-------|-------|------|-------|
| 1 | 0.05 | 0.10 | 0.10 | ✓ | ✓ |
| 2 | 0.10 | 0.10 | 0.10 | ✓ | ✓ |
| 3 | 0.15 | 0.10 | 0.10 | ✓ | ✓ |
| 4 | 0.20 | 0.10 | 0.10 | ✓ | ✓ |
| 5 | 0.25 | 0.10 | 0.10 | ✓ | ✓ |

Air flow $V_x = 9 \text{ m/s}$
 $V_y = 0$
 $V_z = 0$

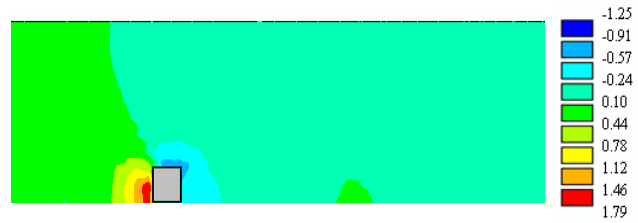
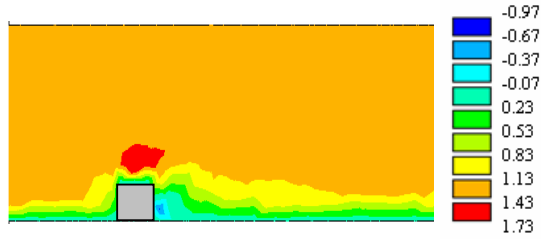
Theoretical model boundary conditions:
 $V_x = 0 \text{ m/s}$
 $V_y = 0$
 $V_z = 0$

Pressure = 0

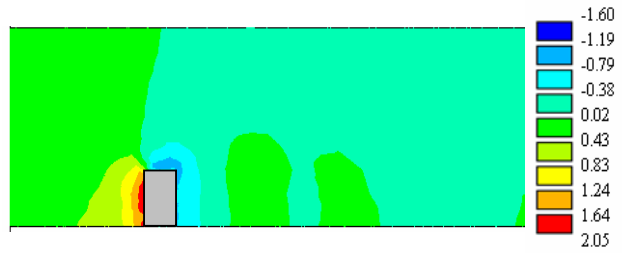
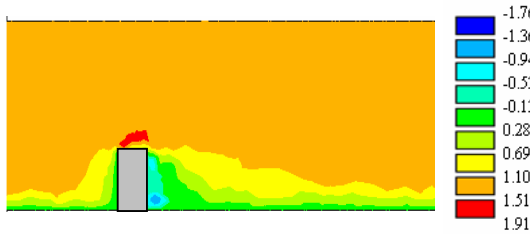
Fig. (5): The theoretical model and its boundary conditions.



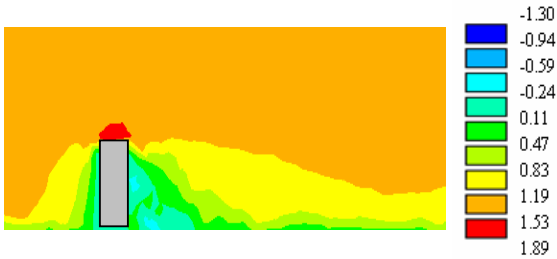
H = 0.05 m



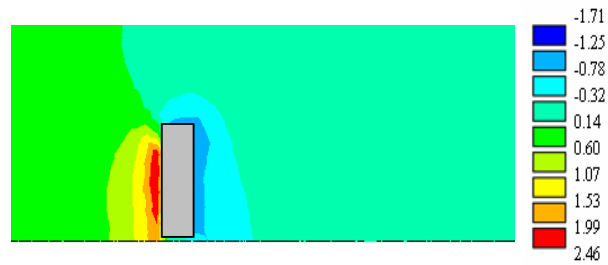
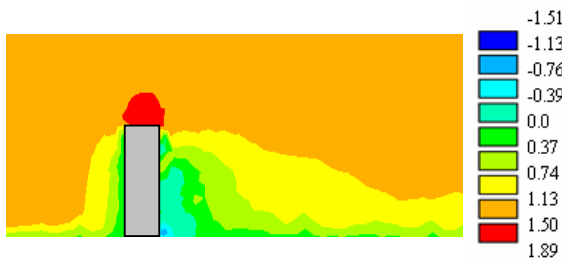
H = 0.10 m



H = 0.15 m



H = 0.20 m

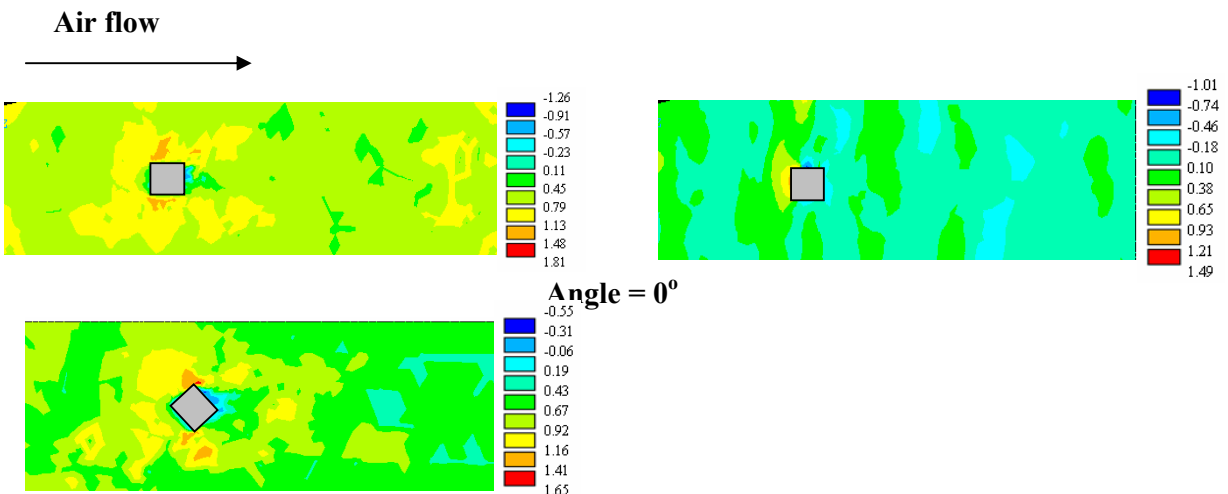


H = 0.25 m

(V/V_∞)

(C_p)

Fig. (6) : Velocity (V/V_∞) and pressure contours (C_p) for different buildings models of different height (side view).



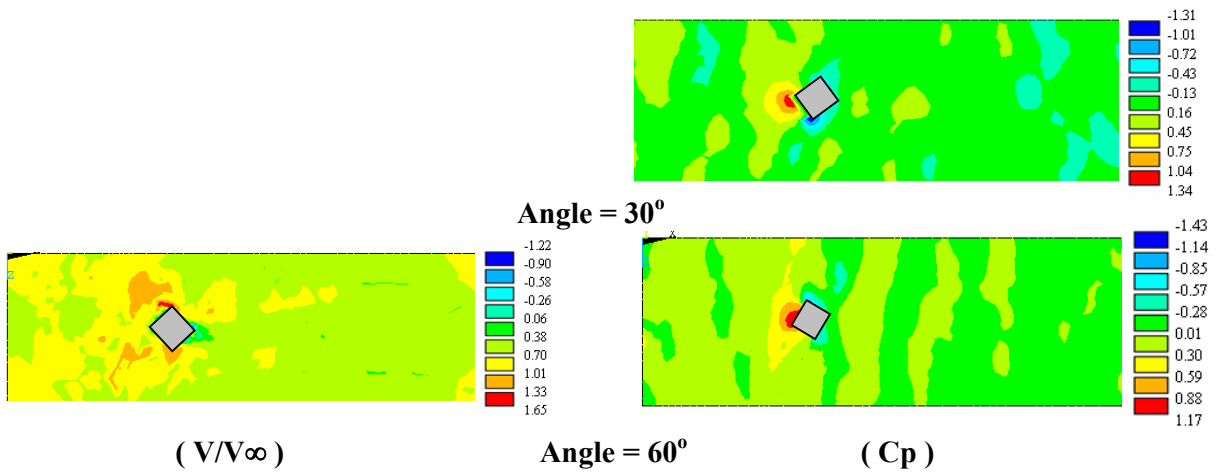


Fig. (7) : Velocity (V/V_∞) and pressure contours (C_p) for different buildings orientation , $H= 0.05$ m (Top view)

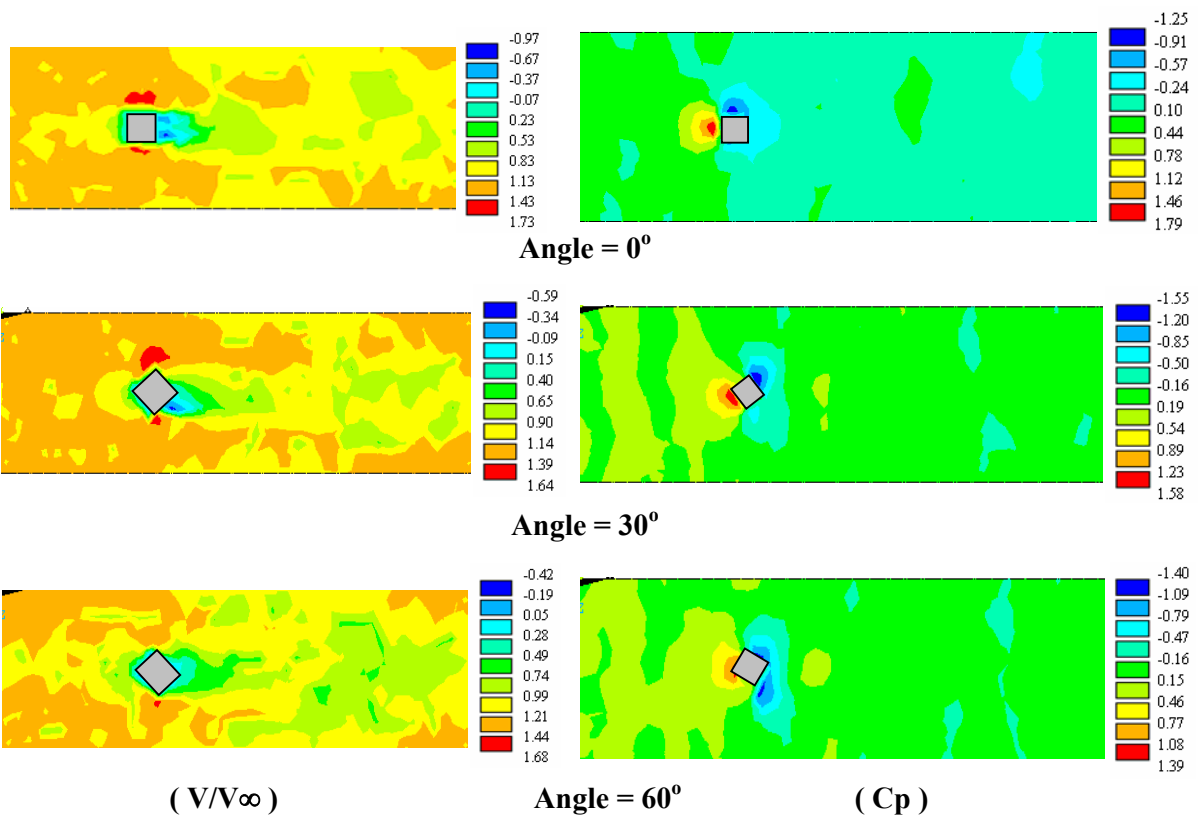
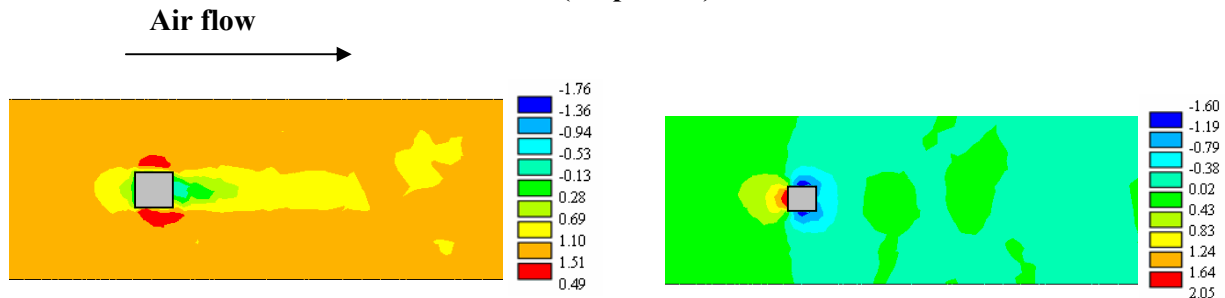


Fig. (8) : Velocity (V/V_∞) and pressure contours (C_p) for different buildings orientation , $H= 0.10$ m (Top view)



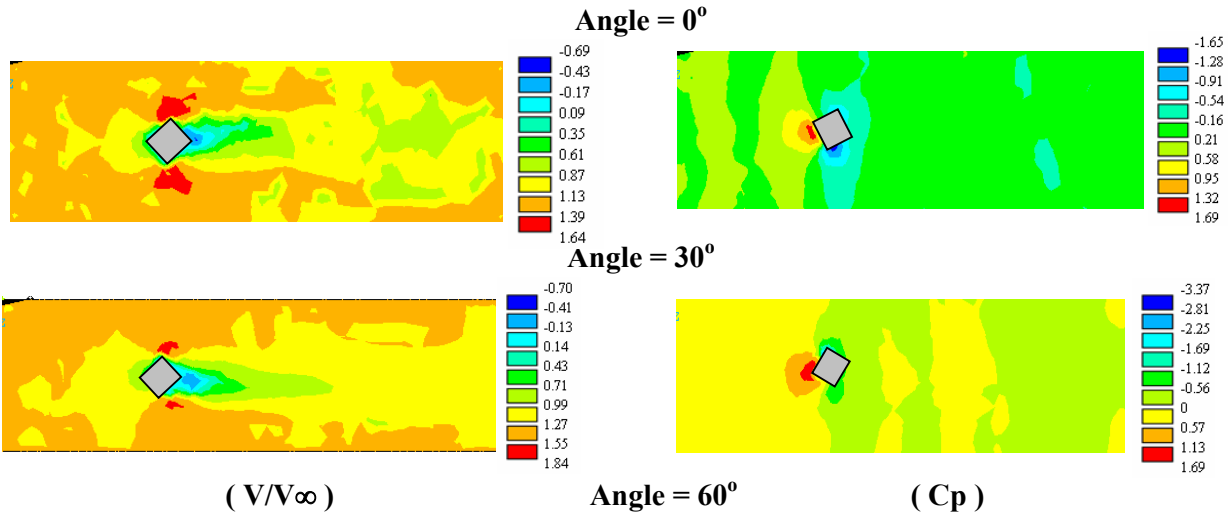


Fig. (9) : Velocity (V/V_∞) and pressure contours (C_p) for different buildings orientation , $H= 0.15$ m (Top view)

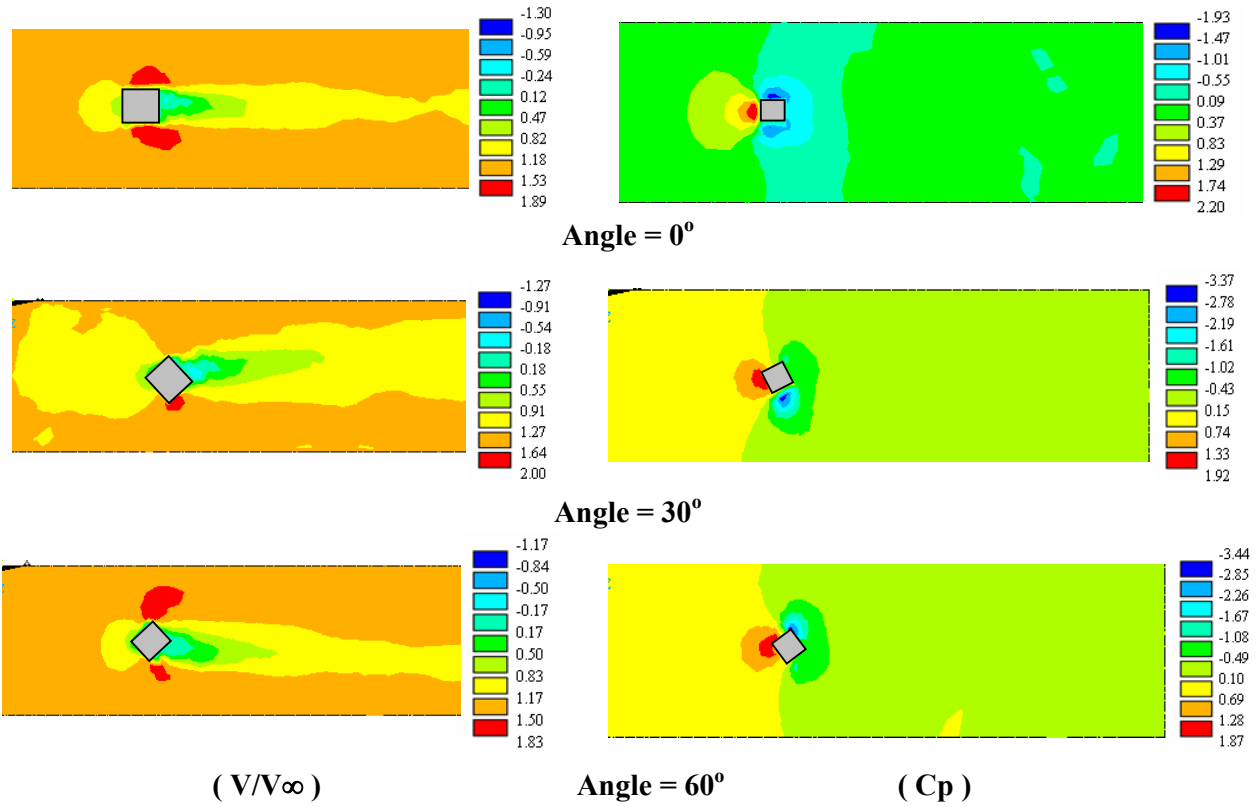
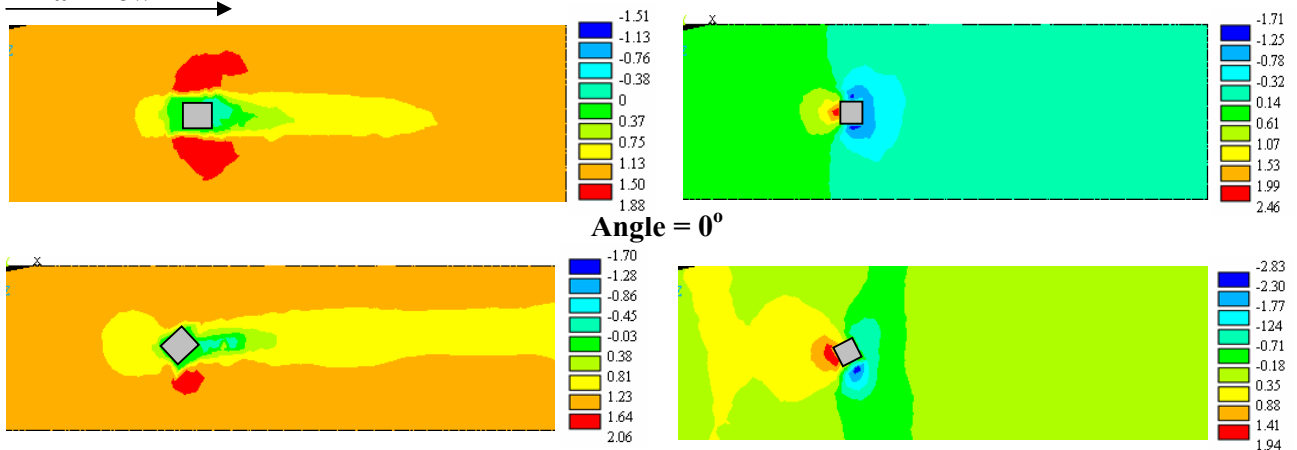


Fig. (10) : Velocity (V/V_∞) and pressure contours (C_p) for different buildings orientation , $H= 0.20$ m air flow



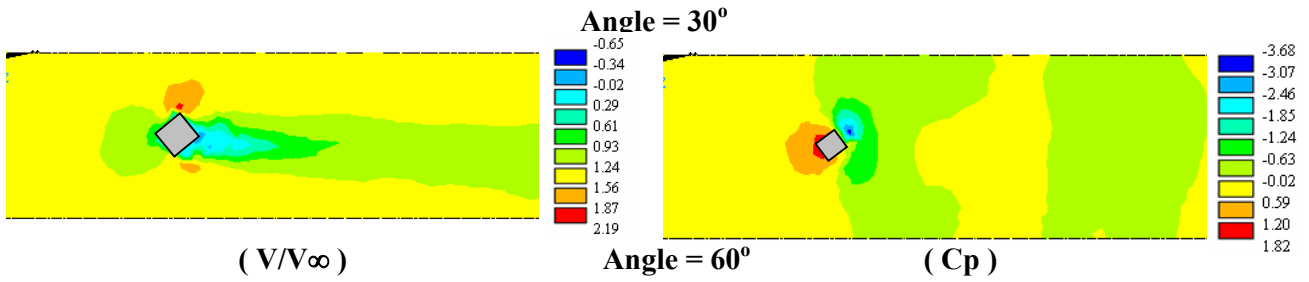
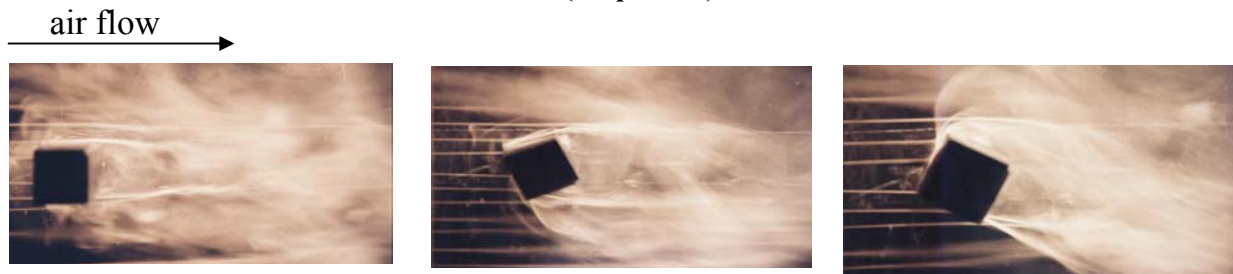
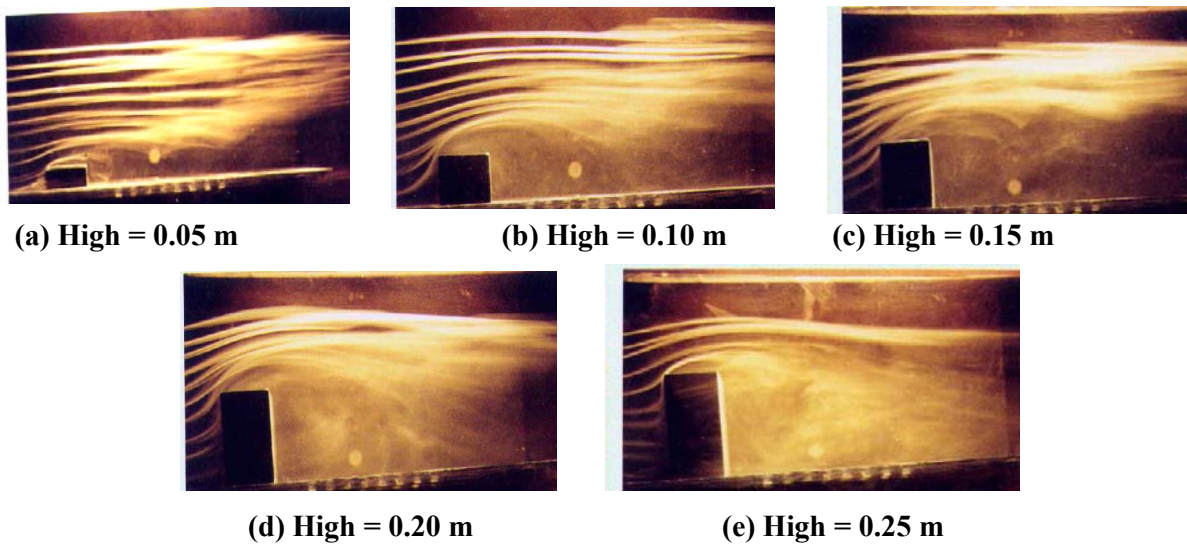


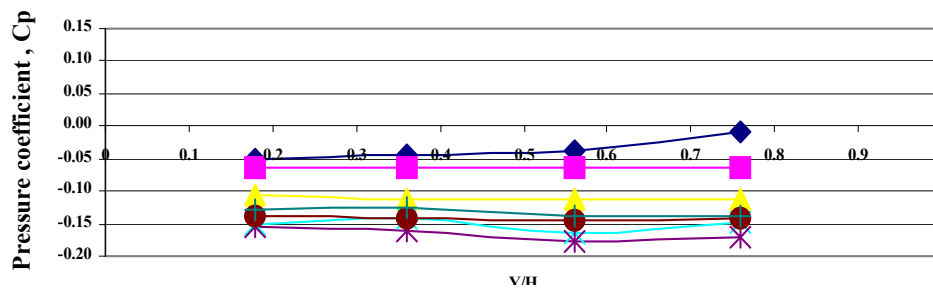
Fig. (11) : Velocity (V/V_∞) and pressure contours (C_p) for different buildings orientation , $H= 0.25$ m (Top view)



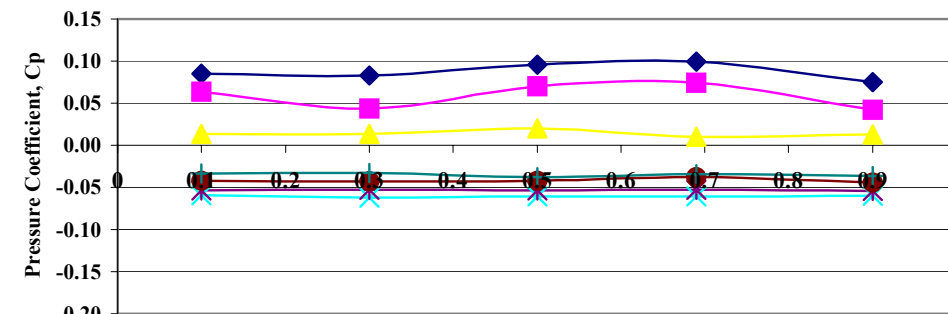
(a) Angle 0° (b) Angle 30° (c) Angle 60°
 Fig. (12) : Visualization of flow around single building models, $v=2$ m/s (Top view)



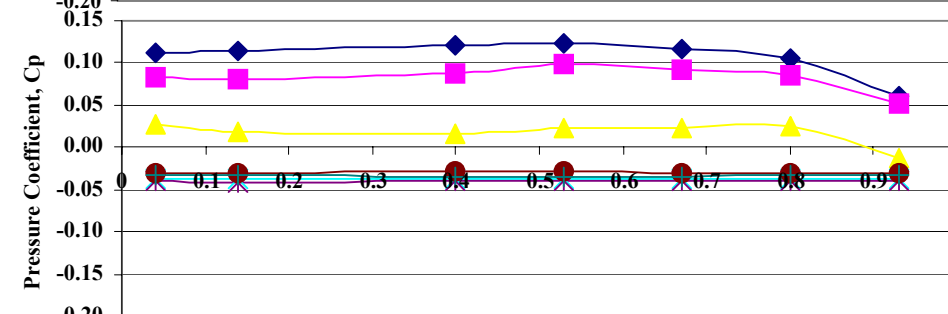
(a) High = 0.05 m (b) High = 0.10 m (c) High = 0.15 m
 (d) High = 0.20 m (e) High = 0.25 m
 Fig. (13): Visualization of flow around single building models $v=2$ m/s (side view).



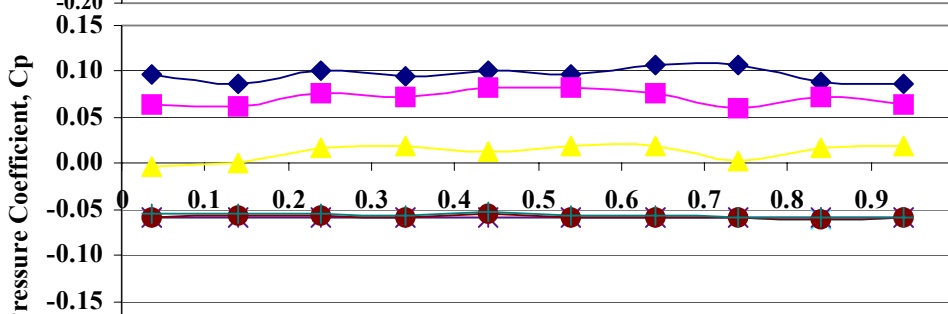
H= 0.05 m



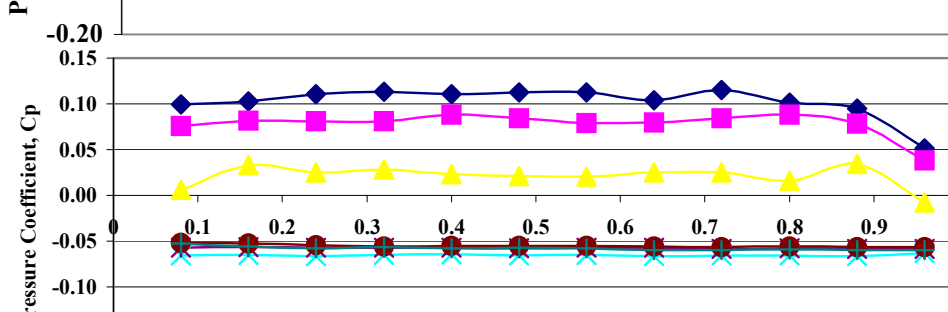
H = 0.10 m



H = 0.15 m



H = 0.20 m



H = 0.25 m

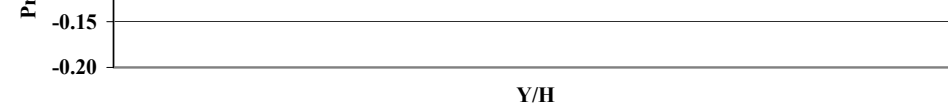


Fig.(14) : Centerline pressure coefficient for different wind angle and different heights.

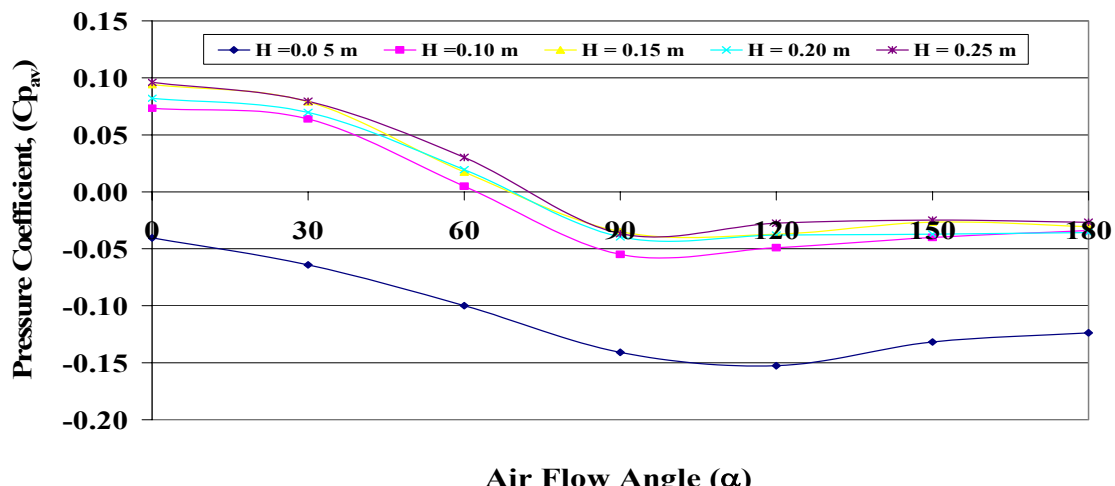


Fig.(15): Pressure coefficient for different building height.

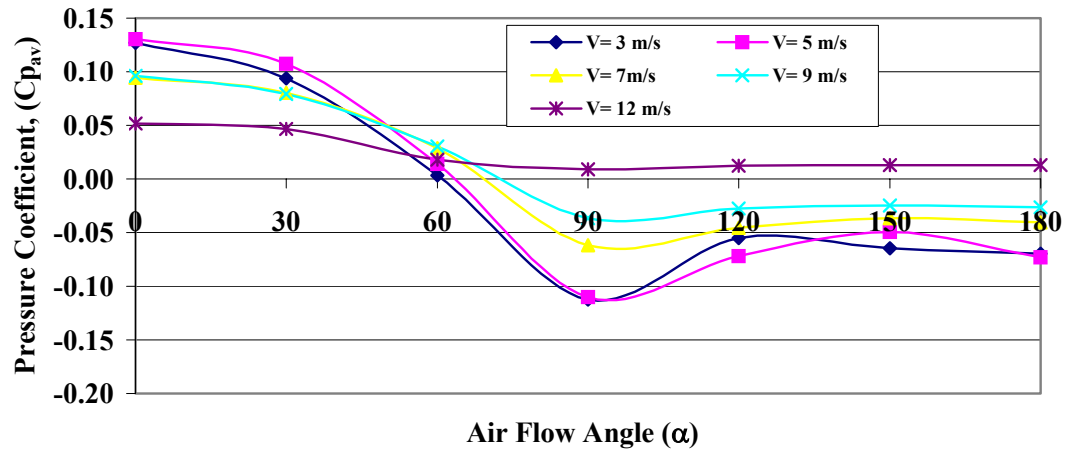


Fig.(16): Pressure coefficient for different values of air velocity, $H = 0.25$ m.

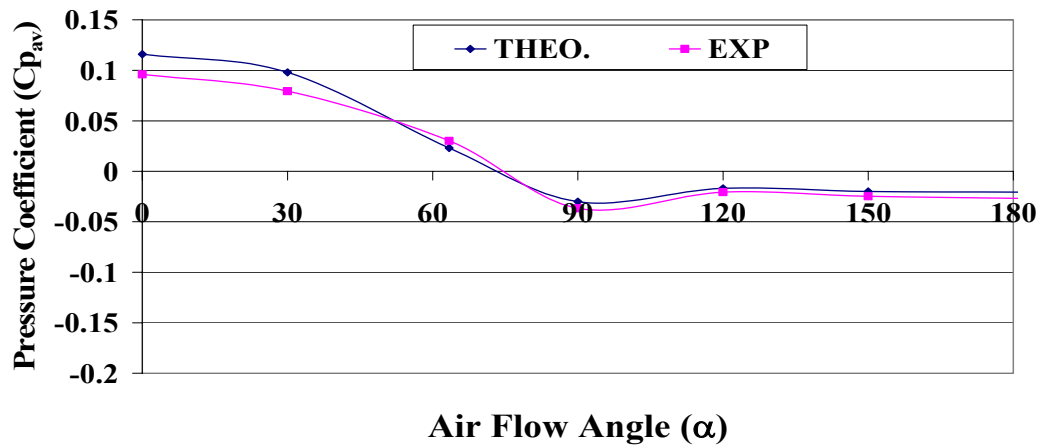


Fig. (17): Comparison between theoretical and experimental results for $c_{p_{av}}$, $H = 0.25$ m .